Enhanced WiFi CSI Fingerprints for Device-Free Localization With Deep Learning Representations

Jianqiang Xue, Jie Zhang, *Member, IEEE*, Zhenyue Gao, and Wendong Xiao, *Senior Member, IEEE*

***Abstract*—With the increasing demands for location-based services in the indoor environments and the widespread deployment of WiFi devices, WiFi-based indoor localization techniques have attracted more attention, especially the device-free localization (DFL), which could estimate the location of the target without attaching any dedicated electronic devices. However, existing fingerprint-based DFL methods face the fingerprint similarity problem, which happens when some fingerprints corresponding to different locations are very similar and may result in the ambiguity in online location estimation phase where we cannot match the fingerprint of the target with the correct one, and severely degrades the localization performance. To address this problem, this article proposes a novel DFL method, in which the original fingerprints are replaced by the hidden layer parameters of the deep neural network. Specifically, the extracted raw data are first transformed into a discriminable feature space using the weights of multilayer extreme learning machine (ML-ELM). Next, we take the generated features as the fingerprints to build an ELM-based DFL model. Finally, we implement a prototype system and evaluate its performance in several indoor environments. Experimental results demonstrate the accuracy and robustness of the proposed method.**

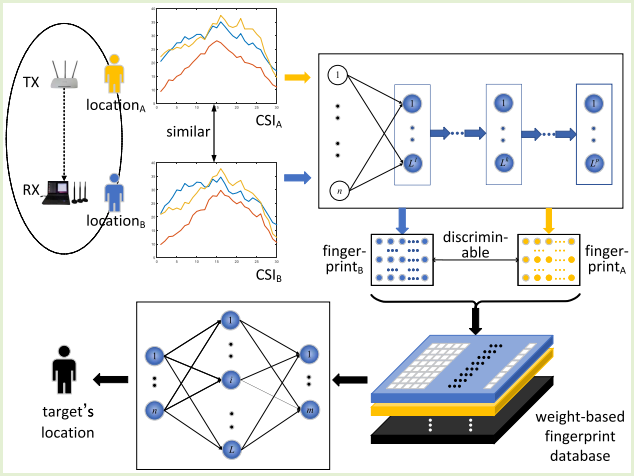

***Index Terms*—Deep learning representations, device-free localization (DFL), fingerprint similarity problem, multilayer extreme learning machine (ML-ELM).**

I. Introduction

IN THE past decade, with the rapid development of the Internet of Things (IoT) infrastructures, location-based services are becoming indispensable and provide great convenience for various applications, ranging from elderly care, smart home, to navigation [1], [2]. In the outdoor environments, target's location information could be achieved with global positioning system (GPS) or base stations. However, in the indoor environments, it is difficult to achieve high accuracy with such manners, because signals from the satellite and base station are seriously attenuated due to the blocking of buildings [3]. In addition, signal propagation is interfered by the rich multipath of indoor environments, leading to low accuracy and poor robustness of the existing indoor localization methods. Therefore, it is of great significance to develop high-accuracy localization methods to enhance the location-based services in the indoor environment.

Indoor localization can be grouped into active localization and passive localization [4], [5]. Active localization requires the target to equip with dedicated electronic devices [6], [7], [8]. Differently, passive localization, also called device-free localization (DFL), can estimate the target's location without the requirement of dedicated electronic devices. According to [9], there is a wide range of commonly used

Manuscript received 29 November 2022; accepted 13 December 2022. Date of publication 29 December 2022; date of current version 31 January 2023. This work was supported in part by the National Natural Science Foundation of China under Grant 62173032 and Grant 62003038, in part by the Foshan Science and Technology Innovation Special Project under Grant BK22BF005, and in part by the Regional Joint Fund of the Guangdong Basic and Applied Basic Research Fund under Grant 2022A1515140109. The associate editor coordinating the review of this article and approving it for publication was Dr. Hassen Fourati. *(Corresponding author: Wendong Xiao.)*

Jianqiang Xue and Zhenyue Gao are with the School of Automation and Electrical Engineering, University of Science and Technology Beijing, Beijing 100083, China (e-mail: b20170301@xs.ustb.edu.cn; 1120461992@qq.com).

Jie Zhang is with the School of Electronic and Electrical Engineering, University of Leeds, LS2 9JT Leeds, U.K. (e-mail: eenjz@leeds.ac.uk).

Wendong Xiao is with the School of Automation and Electrical Engineering, University of Science and Technology Beijing, Beijing 100083, China, also with the Beijing Engineering Research Center of Industrial Spectrum Imaging, Beijing 100083, China, and also with the Shunde Innovation School, University of Science and Technology Beijing, Foshan 528399, China (e-mail: wdxiao@ustb.edu.cn).

Digital Object Identifier 10.1109/JSEN.2022.3231611

DFL techniques, such as ZigBee, radio frequency identification (RFID), camera, ultrasonic, and WiFi. In specific, ZigBee and RFID-based methods usually require dense deployment, seriously limiting their practicality in real settings. The camera-based method involves privacy concerns and its performance highly depends on the lighting condition of the monitoring area. Moreover, the coverage of the ultrasonic-based method is limited. Compared with the aforementioned techniques, the WiFi-based DFL method is more convenient and simpler implementation with the ubiquitous deployment of WiFi-enabled IoT infrastructures [10], [11], [12].

Early WiFi-based DFL methods use received signal strength indicator (RSSI) as the base signal. However, RSSI is actually the superposition value of multiple wireless path signals, and with unpredictable fluctuations even without target locating in the monitoring area [13]. In recent years, with the release of CSITOOL [14], it is possible to obtain channel state information (CSI) from commodity WiFi devices. As fine-grained physical layer information, CSI portrays the multipath information during the wireless signal propagation between the WiFi transmitter and the receiver and has high sensitivity to channel variations [15]. These characteristics enable WiFi CSI-based DFL to be high accuracy.

The WiFi-based DFL could be divided into model-based and fingerprint-based methods [16]. To be specific, the model-based methods usually construct physical models for location estimation by analyzing the relationship between WiFi signal variation and target's location. However, assumptions of physical models in free space cannot be held in practical settings due to the complex layouts and rich multipath of the real environment, degrading the localization performance. Moreover, the fingerprint-based methods first build localization model using machine/deep learning algorithms with fingerprints of the target locating at known locations. Such set of solutions attracts more attentions due to its simpler implementation. The localization performance of the fingerprint-based methods highly depends on the fingerprint, and high-quality fingerprints are helpful for localization performance improvement and vice versa. Observed from the collected data, we find that some fingerprints corresponding to the different target's locations have a certain degree of similarity, which is defined as the fingerprint similarity problem in this article. Fig. 1 depicts the similarity of fingerprints of a specific indoor environment quantified by dynamic time warping (DTW), where many RPs with different locations have very low difference. When such kind of fingerprints is fed into the machine/deep learning algorithms, it is difficult to build a good localization model. Because the machine/deep learning-based DFL model could achieve satisfactory localization performance under the assumption that different locations have different and distinguishable fingerprints. Many progresses have been made by the existing DFL methods for fingerprint enhancement. For example, Li et al. [17] combined the CSI amplitudes and 2-D physical locations to form a matrix to enhance the localization performance by exploiting the correlation between the CSI measurements and physical space. Wu et al. [18] used the mean and standard deviation of the CSI to strengthen

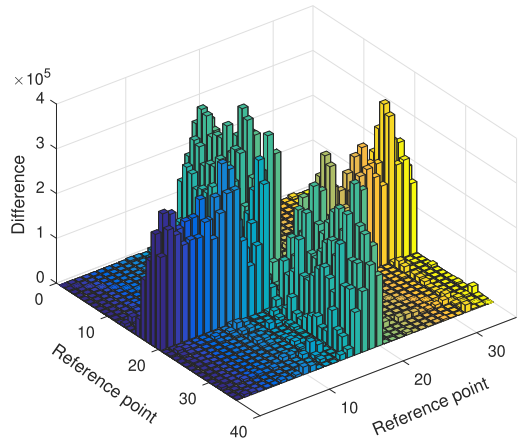

Fig. 1. Fingerprint similarity of different RPs. Both the *X*- and *Y*-axis indicate the serial numbers of RPs and the *Z*-axis depicts the difference in fingerprints between RPs.

the fingerprint quality. Moreover, they used the visibility graph method to explore the correlations of subcarriers with neighboring frequencies instead of considering the correlations of the time series variables [19]. However, they are focusing on how to reduce the effects of multipath without considering the fingerprint similarity problem.

To address the above issue, a novel DFL scheme is developed based on a noniterative deep learning method, named multilayer extreme learning machine (ML-ELM). The proposed ML-ELM-based scheme includes two phases, including the offline phase and the online phase. In specific, during the offline phase, raw CSI data are first extracted from commodity WiFi devices and then fed into an ML-ELM, which is stacked by several ELM autoencoders (ELM-AEs). Different from the existing methods, we use the hidden layer parameters of ML-ELM as the fingerprints. Because the hidden layer parameters contain target's location information after trained using the collected CSI data. Finally, these transformed fingerprints are used to build an ELM-based DFL model. In the online phase, the target's location can be estimated by putting the real-time CSI measurements into the created DFL model. In this manner, transformed fingerprints significantly reduces the effects of fingerprint similarity, and the created DFL model is more robust.

The rest of this article is organized as follows. Related works are reviewed in Section II. Section III presents the relevant fundamentals. The proposed deep-learning-based DFL scheme is described in Section IV. Performance validation is presented in Section V. Finally, we conclude this work in Section VI.

II. Related Work

Location estimation in indoor environments is challenging, but high-accuracy DFL is still expected. Numerous methods have been proposed to achieve accurate and robust DFL, which can be grouped as the model-based and fingerprint-based methods.

A. Model-Based DFL

The model-based DFL methods usually rely on the measured or calculated geometric metrics to estimate the target's location. For example, Qian et al. [11] developed a unified model based on the physical quantities of angle of arrival (AoA), time of arrival (ToA), and Doppler shift and designed a pipeline to translate the erroneous raw parameters into precise locations. Wang et al. [20] designed E-HIPA, an energy-efficient framework for multitarget DFL, which could achieve high localization accuracy only with small amount of RSSI due to compressive sensing. Moreover, they also proposed a modified CSI preprocessing method to refine the subcarriers and estimated the target's location based on the power fading model [21]. To enhance the robustness of DFL, DeFi was proposed, which could reduce the static paths with a background elimination method and separate out the reflection path caused by the target from the dynamic paths based on the AoA and equivalent time-of-flight (ToF) measurements [22]. In this manner, DeFi could achieve satisfactory localization performance using CSI. MFDL proposed a generalized Fresnel penetration model that revealed the linear relationship between specific Fresnel zones and the multicarrier Fresnel phase difference, and then inferred the target's location based on the Fresnel zone sensing theory [23]. Although the model-based DFL methods can characterize the geometric relationship between target's location, signal variations, and physical space, some assumptions may not be held in practical settings, degrading the robustness and generalization. For example, the power fading model and Fresnel penetration model may be seriously distorted by the multipath of the environment, which seriously degrades the localization performance.

B. Fingerprint-Based DFL

The fingerprint-based DFL method is another set of solutions for DFL, which usually uses the difference in the received signal patterns to match the target's location. The fingerprint-based method consists of two stages, including the offline stage and the online stage. In the offline stage, signal variations caused by the target are first collected to build a radio map, while the target's location can be estimated using the real-time signal measurements to match the fingerprint in the created radio map. For example, Zhou et al. [24] first used the density-based spatial clustering method to eliminate the noise in CSI measurements, and the principal component analysis (PCA) was considered to extract the most contributing features. Finally, the support vector machine (SVM)-based DFL model was built with the denoised signals. To implement large-scale DFL, Zhang et al. [25] first divided the whole environment into a number of subdomains by the K-means clustering method, and then trained the corresponding number of DFL models for each subdomain using Fresnel phase difference as the fingerprints. In this way, the large-scale DFL problem can be regarded as conventional DFL problems. Liu et al. [26] proposed a parallel AdaBoost DFL method, which combined multiple naive Bayes classifiers into two strong classifiers. The weighting parameters of those classifiers were then determined based on the learning strategy, and the results of the weighted classifiers were fused to improve the localization performance. Fang et al. [27] focused on using both the properties of amplitude and phase to form hybrid features, and then used deep neural networks to compensate the amplitude and phase for each other. The hybrid features provided an enhanced description of CSI and achieved better accuracy for human detection even with fewer data samples. Li and Rao [28] developed an adaptive deep neural network (AdaptDNN), which used meat-network learning to determine which layers and features of the deep neural network need to be transferred to automatically adapt to the CSI changes. In addition, CSI measurements were transformed into a radio image, and a deep neural network was then applied to extract color and texture features from the constructed radio images [29]. The target's location could be achieved using a machine learning method according to the extracted high-level features. Rao et al. [30] proposed a transfer deep supervised neural network method, combining deep neural network with transfer learning to obtain feature representations as fingerprints. An estimation of the target's location was then obtained using an SVM-based DFL model. Ngamakeur et al. [31] discussed existing works on the fingerprint-based DFL methods and the factors that affect localization accuracy, but ignored the fingerprint similarity problem. Compared with the model-based methods, the fingerprint-based methods are more attractive due to their simpler implementation, which mainly consider the input–output mappings. However, the fingerprint similarity problem may impose serious effects on the localization performance.

III. Preliminaries

In this section, we introduce CSI and ELM theory to help understand the proposed method.

A. CSI Primer

The IEEE802.11a/g/n wireless local area network (LAN) standard protocol is entering our daily life due to the orthogonal frequency division multiplexing (OFDM). OFDM is to divide the data stream into multiple substreams and then modulate these substreams into the corresponding orthogonal subchannels for parallel transmission, which can be used to solve the difficulties in multicarrier transmission systems [32], [33]. It allows the CSI can be parsed from the physical layer between the transmitter and the receiver of commodity WiFi devices. CSI describes the fading of the radio signal during propagating in the physical space, which measures the amplitude and phase information of each subcarrier in the frequency domain.

In a channel with flat fading, the vector at the receiver can be expressed as

$$\mathbf{R} = \mathbf{ZO} + \mathbf{u} \tag{1}$$

where $\mathbf{O}$ is the transmitter vector, $\mathbf{R}$ is the receiver vector, and $\mathbf{u}$ is the noise vector. $\mathbf{Z}$ denotes the CSI, which can be approximated as follows:

$$\mathbf{Z} = \frac{\mathbf{R}}{\mathbf{O}} \tag{2}$$

where fractional notation means the division operation.

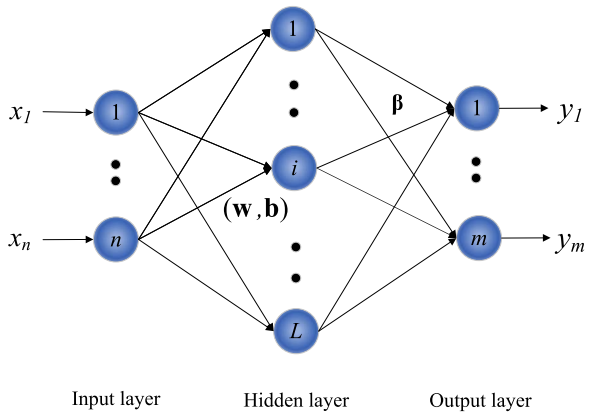

Fig. 2. Main architecture of ELM.

According to (2), the estimated channel information could be obtained at the receiver, and $\mathbf{Z}$ is the channel frequency response sampling information. A single CSI represents the amplitude and phase of an OFDM subcarrier

$$Z(f_s) = \sum_{i=1}^{M} A_i * e^{-j2\pi f_s \tau_i} \tag{3}$$

where j is the imaginary unit, f_s denotes the frequency of the sth subcarrier, τ_i denotes the signal time delay caused on the ith path, A_i represents the amplitude attenuation caused on the ith path, and M denotes the total number of paths propagated by the WiFi signal, respectively.

B. ELM Theory

ELM is a single-hidden layer feedforward network with random input weights and biases, where only the output weights need to be calculated by the least-squares method. Thus, compared with the state-of-the-art methods, ELM has faster learning speed and better generalization performance [34]. Fig. 2 shows the main architecture of ELM, where $\mathbf{x}$ denotes the input, $\mathbf{y}$ is the corresponding output, $\mathbf{w}$ is the input weights, $\mathbf{b}$ is the biases, and $\boldsymbol{\beta}$ denotes the output weights. Mathematically, for N arbitrary distinct samples $\{(\boldsymbol{x}_k, \boldsymbol{y}_k)\}_{k=1}^{N} \subset R^n \times R^m$ and L hidden nodes, where $\boldsymbol{x}_k$ is an n-dimensional input vector and $\boldsymbol{y}_k$ is the corresponding m-dimensional observation vector, the output of ELM can be achieved

$$\sum_{i=1}^{L} \beta_i g_i(\mathbf{x}) = \sum_{i=1}^{L} \beta_i g(\mathbf{w}_i \cdot \mathbf{x} + b_i) = \mathbf{y} \tag{4}$$

where g denotes the activation function.

The compact format of (4) is

$$\mathbf{H}\boldsymbol{\beta} = \mathbf{Y} \tag{5}$$

where

$$\mathbf{H} = g(\mathbf{x}; \mathbf{w}, \mathbf{b}) = \begin{bmatrix} g(\mathbf{w}_1^{\mathrm{T}}\mathbf{x}_1 + b_1) & \cdots & g(\mathbf{w}_L^{\mathrm{T}}\mathbf{x}_1 + b_L) \\ \vdots & \vdots & \vdots \\ g(\mathbf{w}_1^{\mathrm{T}}\mathbf{x}_N + b_1) & \cdots & g(\mathbf{w}_L^{\mathrm{T}}\mathbf{x}_N + b_L) \end{bmatrix}_{N \times L}. \tag{6}$$

To improve the robustness and generalization of ELM, regularized ELM (R-ELM) was proposed [35], [36], where a user-specified parameter is used to balance the empirical risk and structural risk

$$\min \lambda_{\mathrm{RELM}} = \frac{1}{2}\|\boldsymbol{\beta}\|^2 + \frac{C}{2}\|\mathbf{Y} - \mathbf{H}\boldsymbol{\beta}\|^2 \tag{7}$$

where C is a parameter to balance the empirical risk and structural risk.

By setting the gradient of λ_{RELM} to zero, we have

$$\boldsymbol{\beta} - C\mathbf{H}^{\mathbf{T}}(\mathbf{Y} - \mathbf{H}\boldsymbol{\beta}) = 0. \tag{8}$$

When the number of training samples is larger than the number of hidden nodes, the output weight matrix $\boldsymbol{\beta}$ can be expressed as

$$\boldsymbol{\beta} = \left(\frac{\mathbf{I}}{C} + \mathbf{H}^T\mathbf{H}\right)^{-1}\mathbf{H}^T\mathbf{Y}. \tag{9}$$

When the number of training samples is less than the number of hidden nodes, the output weight matrix $\boldsymbol{\beta}$ is

$$\boldsymbol{\beta} = \mathbf{H}^T\left(\frac{\mathbf{I}}{C} + \mathbf{H}\mathbf{H}^T\right)^{-1}\mathbf{Y}. \tag{10}$$

IV. Methods

In this section, we first analyze the fingerprint similarity in DFL to formulate the problem description. The main framework and details of the proposed method are then demonstrated, respectively.

A. Problem Description

The localization performance of the fingerprint-based DFL method highly depends on the quality of the constructed fingerprints. The CSI measurements of a pair of WiFi transceivers are usually affected by several factors, such as the energy attenuation caused by WiFi signal propagation, the reflected signal added by the entry of the localized target, the small signal variations due to the multipath, and unknown noise, and thus, the signal patterns corresponding to specific locations may not be consistent. Without loss of generality, we take the CSI amplitude as an example to demonstrate the empirical study for the fingerprint similarity problem. As shown in Fig. 3(a), in a specific indoor environment with a pair of WiFi transceiver deployed, when a target moves from the inside to the outside along the vertical bisector of the Fresnel zones (denoted by the red and blue lines), the received WiFi signals will show a sinusoidal-like wave, and the number of peaks and valleys indicates the number of the Fresnel zones the target crosses [37]. Fig. 3(b) illustrates the signal variations in the denoised CSI, from which we can find that some peaks and valleys have similar CSI amplitude values, such as the ones pointed out by red and green circles. It means that the fingerprint may be similar even when the target localizes at different locations, which may seriously degrade the localization performance [38]. Accordingly, it is worthwhile to address the fingerprint similarity issue to enhance the quality of the fingerprint.

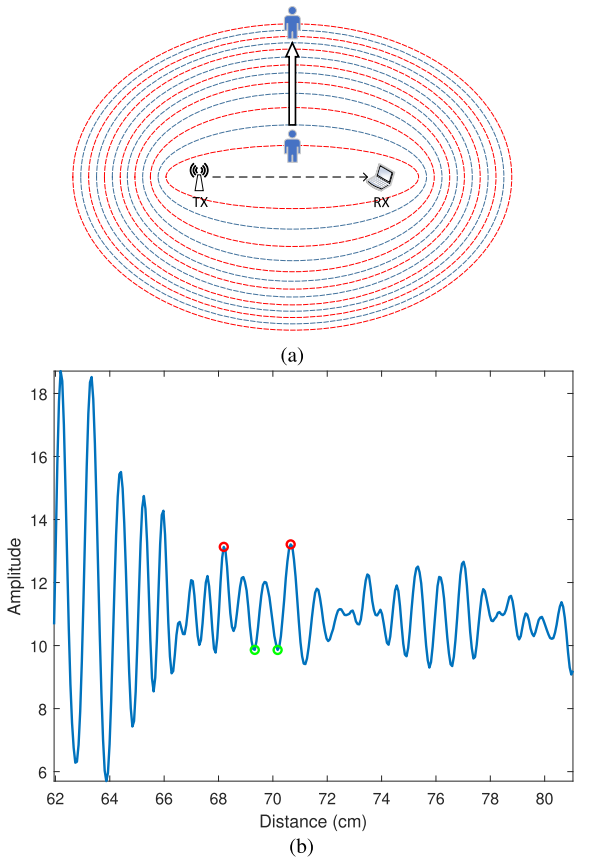

Fig. 3. Empirical study of the fingerprint similarity. (a) Target walks along the vertical bisector. (b) Illustration of the received WiFi signals.

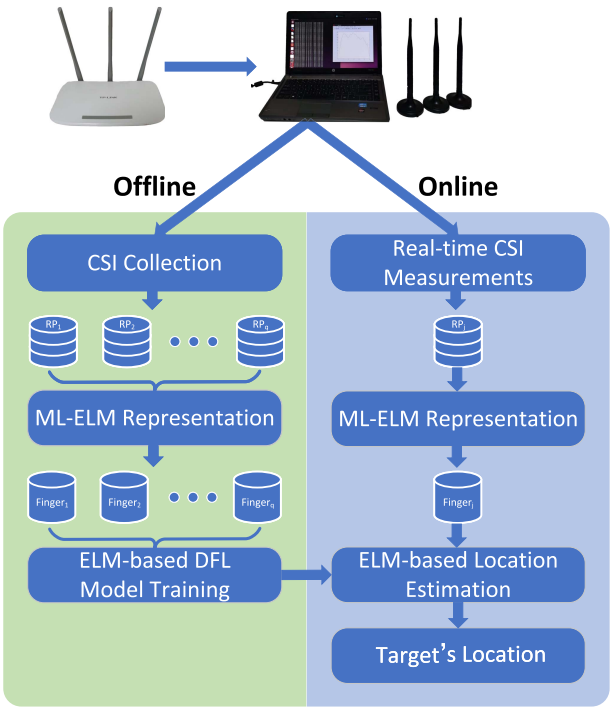

Fig. 4. Main framework of the ML-ELM-based DFL.

B. Main Framework of ML-ELM-Based DFL

Fig. 4 shows the main framework of the proposed ML-ELM-based DFL, which consists of two phases, including the offline phase and the online phase. In the offline phase, CSI measurements are received by the WiFi receiver, and then the collected data are fed into an ML-ELM with several hidden layers to generate the weight-based fingerprints to reduce the effects of the fingerprint similarity on the localization performance. To be specific, we use the hidden layer parameters of the trained ML-ELM to replace the raw CSI measurements as the fingerprints (more details of the weight-based fingerprint generated process are shown in Algorithm 1). Because ML-ELM is trained using CSI measurements, its hidden layer parameters contain the location information of the target. CSI measurements collected from each RP are fed into ML-ELM to achieve the corresponding weight-based fingerprints. Finally, a new kind of fingerprints generated from all the RPs is applied to build an ELM-based DFL model. In the online phase, after the WiFi receiver receives the new CSI signals, they are first transformed as the weight-based fingerprints, and then the target's location can be estimated through the DFL model trained in the offline phase.

C. Deep Learning Representations for Fingerprint Enhancement

Autoencoder (AE) is an unsupervised neural network, commonly used in deep learning to stack the deep neural network, whose output equals the input. Similar to the conventional AE, the ELM-AE model consists of an input layer, a hidden layer, and an output layer, whose output is equal to the input [39], [40].

There are two differences between ELM-AE and classic ELM. First, ELM is a supervised neural network and the outputs are the predicted labels, while ELM-AE is an unsupervised neural network and the outputs are equal to the inputs. Moreover, the input weights and the biases of ELM-AE are orthogonal, whereas the hidden layer parameters of ELM are initialized randomly.

The hidden layer output of ELM-AE and the relationship between the hidden layer output and the output layer output can be expressed as follows:

$$\begin{aligned} \mathbf{h} &= g(\mathbf{w}\cdot\mathbf{x}+b), \quad \text{where } \mathbf{w}^{\mathrm{T}}\mathbf{w}=\mathbf{I}, \mathrm{b}^{\mathrm{T}}\mathrm{b}=1 \\ h(\mathbf{x}_i)\boldsymbol{\beta} &= \mathbf{x}_i^T, \quad \text{where } i=1,2,\ldots,N. \end{aligned} \tag{11}$$

The calculation of the output weight of ELM-AE is different from that of ELM. The output weight obtained in ELM-AE is divided into three categories, including the compressed, equal dimension, and sparse representations. For compressed and sparse representations, the output weights are calculated as

$$\boldsymbol{\beta} = \begin{cases} \left(\dfrac{\mathbf{I}}{C}+\mathbf{H}^T\mathbf{H}\right)^{-1}\mathbf{H}^T\mathbf{X}, & N \geq L \\ \mathbf{H}^T\left(\dfrac{\mathbf{I}}{C}+\mathbf{H}\mathbf{H}^T\right)^{-1}\mathbf{X}, & N < L. \end{cases} \tag{12}$$

For equal dimension representations, the output weights can be calculated as follows:

$$\boldsymbol{\beta} = \mathbf{H}^{-1}\mathbf{X}. \tag{13}$$

An ML-ELM with several hidden layers can be obtained by stacking ELM-AEs, as shown in Fig. 5. If the number of

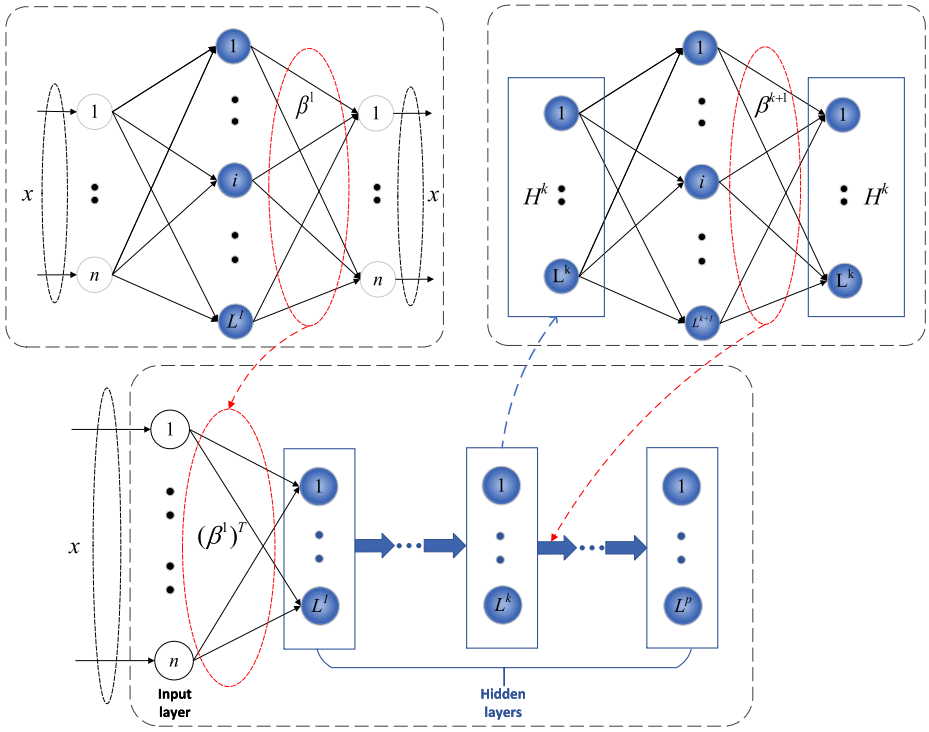

Fig. 5. ML-ELM-based weight-based fingerprint generation.

hidden nodes in the kth hidden layer is equal to the number of hidden nodes in the $(k-1)$th layer, the activation function g is linear; otherwise, g is nonlinear

$$\mathbf{H}^k = g\left(\left(\boldsymbol{\beta}^k\right)^T \mathbf{H}^{k-1}\right) \tag{14}$$

where $\mathbf{H}^k$ is the output matrix of the kth hidden layer. The input layer $\mathbf{x}$ can be considered as the 0th hidden layer, where $k = 0$.

As mentioned above, to reduce the effects of the fingerprint similarity problem on the localization performance, we first use ML-ELM to regenerate the new weight-based fingerprints, in which the location information is embedded in the hidden layer parameters of ML-ELM, and then use these parameters to replace the raw fingerprints (see Algorithm 1).

Algorithm 1 Weight-Based Fingerprint Generation

Input: N packet receptions each with 180 CSI values for each of the q training locations;
Output: q groups of fingerprints corresponding to q locations;

```
for i = 1; i <= q do
    Set H^0 = x, //suppose the input data x as the 0th hidden layer;
    Randomly initialize w, b; //weights and biases are chosen to be orthogonal;
    //p is the number of hidden layers;
    for k = 1; k <= p do
        H = g(wH^{k-1} + b), // g is sigmoid function;
        β^k = (I/C + H^T H)^{-1} H^T H^{k-1};
        H^k = g((β^k)^T H^{k-1});
    end for
    //Obtain Fingerprint_i;
    Fingerprint_i ← [β^1, ··· , β^p];
end for
```

V. Performance Verification

In this section, the performance of the proposed method is verified in three environments, including the activity room, the basement area, and the corridor area, by comparing with several commonly used methods in DFL, including SVM, random forest, decision tree, and back-propagation neural network (BPNN).

A. Experimental Setup

In the experiments, we deploy one WiFi transmitter and one WiFi receiver in each environment, and both the WiFi transmitter and the receiver are with Intel 5300 NICs. The WiFi transmitter is equipped with two antennas and the WiFi receiver is configured with three antennas, enabling it to receive 180 samples per packet. To capture the raw CSI, we use the CSITOOL under Linux system, and the RPs are set to the center of each cell and the testing points are randomly scattered in the monitoring area. We conducted experiments in three different environments, and the details about these experiments are shown in Figs. 6–8, respectively. To better demonstrate the environmental information, we use all the subcarriers in the experiments. It should be noted that

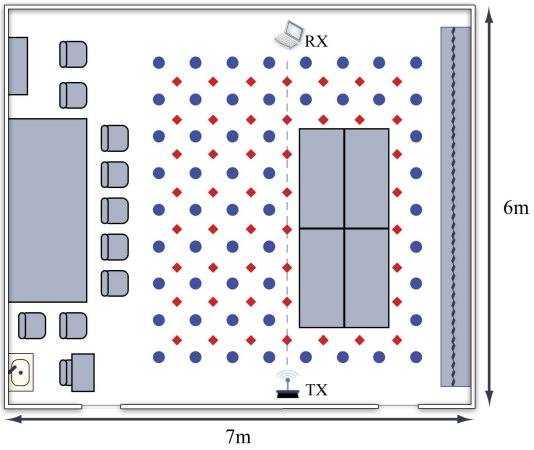

Fig. 6. Layout of the activity room. The blue points are RPs, and the red points are testing points.

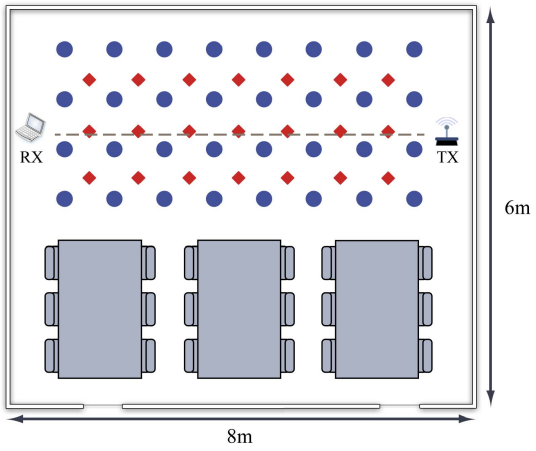

Fig. 7. Layout of the basement area. The blue points are RPs, and the red points are testing points.

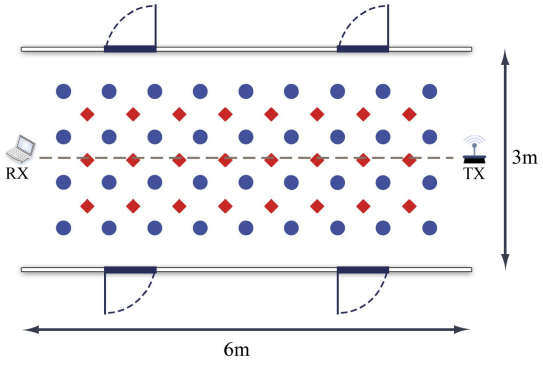

Fig. 8. Layout of the corridor area. The blue points are RPs, and the red points are testing points.

we only use the CSI amplitude due to the randomness and unavailability of the CSI phase.

B. Performance Evaluation of ML-ELM-Based DFL Model

We first verify the effectiveness of the proposed weight-based fingerprint by comparing with some classical fingerprints commonly used in DFL. Specifically, all the raw data are denoised through a Hampel filter, and a moving average filter is then used to remove high-frequency values. Due to the complex indoor environment, data packets may lose during communications and result in missing packets corresponding to the discontinuous time labels. Therefore, we use 1-D linear interpolation to add the missing samples based on the samples before and after the lost ones. The ratio data are the ratio of the CSI data of two antennas, which can eliminate noise and increase the signal-to-noise ratio. The conjugate multiplication data are obtained by conjugate multiplying the CSI data of the two antennas, which can effectively eliminate the effects of the multipath. The experimental results are shown in Table I, from which we can find that the proposed weight-based fingerprints can significantly enhance the localization performance.

TABLE I
EXPERIMENTAL RESULTS BETWEEN THE PROPOSED WEIGHT-BASED FINGERPRINT AND OTHER CLASSIC FINGERPRINTS

Fingerprint Type	Localization Error (m)
Wieght-based fingerprint	1.06
CSI amplitude	1.31
CSI ratio	1.13
Conjugate multiplication data	1.26

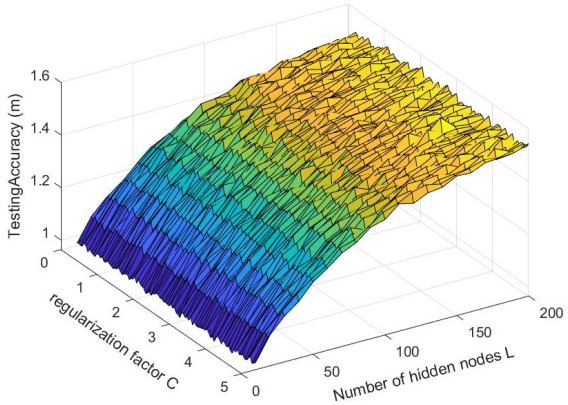

Fig. 9. Effects of the regularization factor C and the number of hidden nodes L.

We then evaluate the effectiveness of the proposed ML-ELM-based DFL method by comparing with other classic methods in DFL. There are two parameters in ELM that need to be adjusted, i.e., the number of hidden nodes L and the regularization factor C. If the fitting ability of the model is stronger, it may be overfitted, so we add regularization parameter to reduce the overfitting problem and use 10-fold cross-validation and grid search methods to determine the optimal parameters. Fig. 9 shows the effects under different hyperparameter values. According to Fig. 9, we can find that the localization accuracy of the proposed method is becoming better with the decrease in the number of hidden nodes of ELM, and it means that we can achieve satisfactory localization performance with few hidden nodes, which could significantly reduce the time consumption

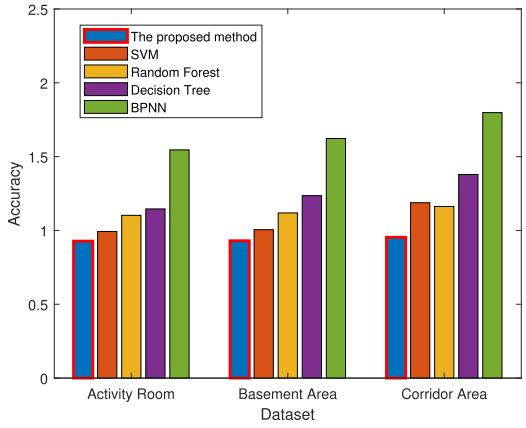

Fig. 10. Comparison results between the proposed method and selected methods.

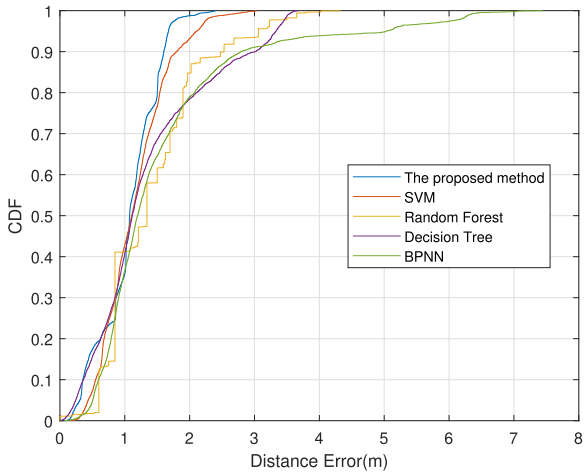

Fig. 11. CDF curves of different methods in the activity room.

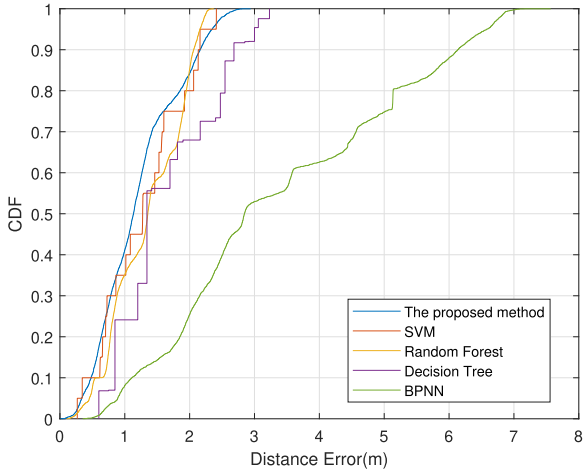

Fig. 12. CDF curves of different methods in the basement area.

of DFL model training. Finally, we set $L = 10$ and $C = 3.85$ in the following experiments.

We use the average distance error as the performance evaluation metric, and the comparison results are shown in Fig. 10. It can be seen that our method outperforms the selected

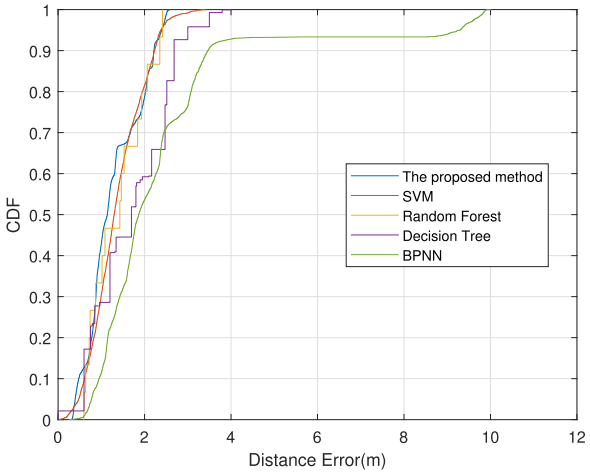

Fig. 13. CDF curves of different methods in the corridor area.

methods in terms of localization accuracy. Furthermore, Fig. 11 illustrates the cumulative distribution function (CDF) of the localization error of the activity room. From Fig. 11, we can see that the localization performance of the proposed method is generally better than other methods. Specifically, the proposed method still can achieve a mean localization error of 1.0 m in the activity room scenario with rich multipath and shadow effects, but the mean localization errors for SVM, random forest, decision tree, and BPNN are worse, and they are 1.2, 1.4, 1.3, and 1.6 m, respectively. We also test the localization performance of these methods in the basement and corridor areas, and the results are shown in Figs. 12 and 13, respectively. Obviously, the proposed method achieves the best localization accuracy in both the environments, which shows the good robustness of the proposed method in different scenarios.

VI. Conclusion

In this paper, we focus on the fingerprint similarity problem in DFL and propose an ML-ELM-based DFL method, in which the hidden layer parameters of ML-ELM are used to represent the raw fingerprints to enhance the localization performance. The experimental results in several indoor scenarios indicate that the proposed method could achieve better localization performance. For the future work, because time-varying characteristics of environments and different device deployments usually lead to changes in the distribution of CSI signals, further study is needed to improve the proposed method under the dynamic localization environment.

References

[1] X. Chen, L. Chen, C. Feng, D. Fang, J. Xiong, and Z. Wang, "Sensing our world using wireless signals," *IEEE Internet Comput.*, vol. 23, no. 3, pp. 38–45, May 2019.

[2] J. Zhang, Y. Li, W. Xiao, and Z. Zhang, "Online spatiotemporal modeling for robust and lightweight device-free localization in nonstationary environments," *IEEE Trans. Ind. Informat.*, early access, Nov. 2, 2022, doi: 10.1109/TII.2022.3218666.

[3] Z. Yang, Z. Zhou, and Y. Liu, "From RSSI to CSI: Indoor localization via channel response," *ACM Comput. Surv.*, vol. 46, no. 2, pp. 1–32, 2013.

[4] B. Lashkari, J. Rezazadeh, R. Farahbakhsh, and K. Sandrasegaran, "Crowdsourcing and sensing for indoor localization in IoT: A review," *IEEE Sensors J.*, vol. 19, no. 7, pp. 2408–2434, Apr. 2018.

[5] J. Zhang, Y. Li, and W. Xiao, "Integrated multiple kernel learning for device-free localization in cluttered environments using spatiotemporal information," *IEEE Internet Things J.*, vol. 8, no. 6, pp. 4749–4761, Mar. 2021.

[6] F. Potortì et al., "Off-line evaluation of indoor positioning systems in different scenarios: The experiences from IPIN 2020 competition," *IEEE Sensors J.*, vol. 22, no. 6, pp. 5011–5054, Mar. 2021.

[7] F. Potorti et al., "The IPIN 2019 indoor localisation competition—Description and results," *IEEE Access*, vol. 8, pp. 206674–206718, 2020.

[8] V. Renaudin, "Evaluating indoor positioning systems in a shopping mall: The lessons learned from the IPIN 2018 competition," *IEEE Access*, vol. 7, pp. 148594–148628, 2019.

[9] R. C. Shit et al., "Ubiquitous localization (UbiLoc): A survey and taxonomy on device free localization for smart world," *IEEE Commun. Surveys Tuts.*, vol. 21, no. 4, pp. 3532–3564, 4th Quart., 2019.

[10] J. Zhang, Y. Li, H. Xiong, D. Dou, C. Miao, and D. Zhang, "HandGest: Hierarchical sensing for robust-in-the-air handwriting recognition with commodity WiFi devices," *IEEE Internet Things J.*, vol. 9, no. 19, pp. 19529–19544, Oct. 2022.

[11] K. Qian, C. Wu, Y. Zhang, G. Zhang, Z. Yang, and Y. Liu, "Widar2.0: Passive human tracking with a single Wi-Fi link," in *Proc. ACM Int. Conf. Mob. Syst., Appl., Serv. (MobiSys)*, 2018, pp. 350–361.

[12] Y. Li et al., "Diversense: Maximizing Wi-Fi sensing range leveraging signal diversity," *Proc. ACM Interact. Mob. Wearable Ubiquitous Technol.*, vol. 6, no. 2, pp. 1–28, 2022.

[13] J. Wang, X. Zhang, Q. Gao, H. Yue, and H. Wang, "Device-free wireless localization and activity recognition: A deep learning approach," *IEEE Trans. Veh. Technol.*, vol. 66, no. 7, pp. 6258–6267, Jul. 2016.

[14] D. Halperin, W. Hu, A. Sheth, and D. Wetherall, "Tool release: Gathering 802.11n traces with channel state information," *ACM SIGCOMM Comput. Commun. Rev.*, vol. 41, no. 1, p. 53, Jan. 2011.

[15] K. P. Nkabiti and Y. Chen, "Application of solely self-attention mechanism in CSI-fingerprinting-based indoor localization," *Neural Comput. Appl.*, vol. 33, no. 15, pp. 9185–9198, Aug. 2021.

[16] Z. Wang, B. Guo, Z. Yu, and X. Zhou, "Wi-Fi CSI-based behavior recognition: From signals and actions to activities," *IEEE Commun. Mag.*, vol. 56, no. 5, pp. 109–115, May 2018.

[17] Q. Li, X. Liao, M. Liu, and S. Valaee, "Indoor localization based on CSI fingerprint by Siamese convolution neural network," *IEEE Trans. Veh. Technol.*, vol. 70, no. 11, pp. 12168–12173, Nov. 2021.

[18] Z. Wu, Q. Xu, J. Li, C. Fu, Q. Xuan, and Y. Xiang, "Passive indoor localization based on CSI and naive Bayes classification," *IEEE Trans. Syst. Man, Cybern., Syst.*, vol. 48, no. 9, pp. 1566–1577, Sep. 2017.

[19] Z. Wu, X. Pan, K. Fan, K. Liu, and Y. Xiang, "Device-free orientation detection based on CSI and visibility graph," *IEEE Trans. Syst., Man, Cybern. Syst.*, vol. 51, no. 7, pp. 4433–4442, Jul. 2019.

[20] J. Wang et al., "E-HIPA: An energy-efficient framework for high-precision multi-target-adaptive device-free localization," *IEEE Trans. Mobile Comput.*, vol. 16, no. 3, pp. 716–729, May 2017.

[21] J. Wang et al., "Low human-effort, device-free localization with fine-grained subcarrier information," *IEEE Trans. Mobile Comput.*, vol. 17, no. 11, pp. 2550–2563, Mar. 2018.

[22] L. Zhang, Q. Gao, X. Ma, J. Wang, T. Yang, and H. Wang, "DeFi: Robust training-free device-free wireless localization with WiFi," *IEEE Trans. Veh. Technol.*, vol. 67, no. 9, pp. 8822–8831, Sep. 2018.

[23] H. Wang et al., "MFDL: A multicarrier Fresnel penetration model based device-free localization system leveraging commodity Wi-Fi cards," 2017, *arXiv:1707.07514*.

[24] R. Zhou, X. Lu, P. Zhao, and J. Chen, "Device-free presence detection and localization with SVM and CSI fingerprinting," *IEEE Sensors J.*, vol. 17, no. 23, pp. 7990–7999, Dec. 2017.

[25] J. Zhang, W. Xiao, and Y. Li, "Data and knowledge twin driven integration for large-scale device-free localization," *IEEE Internet Things J.*, vol. 8, no. 1, pp. 320–331, Jan. 2020.

[26] Z. Liu, D. Liu, J. Xiong, and X. Yuan, "A parallel AdaBoost method for device-free indoor localization," *IEEE Sensors J.*, vol. 22, no. 3, pp. 2409–2418, Feb. 2022.

[27] S.-H. Fang, C.-C. Li, W.-C. Lu, Z. Xu, and Y.-R. Chien, "Enhanced device-free human detection: Efficient learning from phase and amplitude of channel state information," *IEEE Trans. Veh. Technol.*, vol. 68, no. 3, pp. 3048–3051, Mar. 2019.

[28] Z. Li and X. Rao, "Toward long-term effective and robust device-free indoor localization via channel state information," *IEEE Internet Things J.*, vol. 9, no. 5, pp. 3599–3611, Mar. 2022.

[29] Q. Gao, J. Wang, X. Ma, X. Feng, and H. Wang, "CSI-based device-free wireless localization and activity recognition using radio image features," *IEEE Trans. Veh. Technol.*, vol. 66, no. 11, pp. 10346–10356, Nov. 2017.

[30] X. Rao, Z. Li, Y. Yang, and S. Wang, "DFPhaseFL: A robust device-free passive fingerprinting wireless localization system using CSI phase information," *Neural Comput. Appl.*, vol. 32, no. 18, pp. 14909–14927, Sep. 2020.

[31] K. Ngamakeur, S. Yongchareon, J. Yu, and S. U. Rehman, "A survey on device-free indoor localization and tracking in the multi-resident environment," *ACM Comput. Surveys*, vol. 53, no. 4, pp. 1–29, Jul. 2021.

[32] J. Yan, L. Wan, W. Wei, X. Wu, W.-P. Zhu, and D. P.-K. Lun, "Device-free activity detection and wireless localization based on CNN using channel state information measurement," *IEEE Sensors J.*, vol. 21, no. 21, pp. 24482–24494, Nov. 2021.

[33] Y. Duan et al., "Data rate fingerprinting: A WLAN-based indoor positioning technique for passive localization," *IEEE Sensors J.*, vol. 19, no. 15, pp. 6517–6529, Apr. 2019.

[34] J. Zhang, W. Xiao, Y. Li, and S. Zhang, "Residual compensation extreme learning machine for regression," *Neurocomputing*, vol. 311, pp. 126–136, Oct. 2018.

[35] G.-B. Huang, H. Zhou, X. Ding, and R. Zhang, "Extreme learning machine for regression and multiclass classification," *IEEE Trans. Syst., Man, Cybern. B, Cybern.*, vol. 42, no. 2, pp. 513–529, Apr. 2012.

[36] Y. Li, J. Zhang, S. Zhang, W. Xiao, and Z. Zhang, "Multi-objective optimization-based adaptive class-specific cost extreme learning machine for imbalanced classification," *Neurocomputing*, vol. 496, pp. 107–120, Jul. 2022.

[37] D. Zhang, H. Wang, and D. Wu, "Toward centimeter-scale human activity sensing with Wi-Fi signals," *Computer*, vol. 50, no. 1, pp. 48–57, Jan. 2017.

[38] X. Wang, L. Gao, S. Mao, and S. Pandey, "CSI-based fingerprinting for indoor localization: A deep learning approach," *IEEE Trans. Veh. Technol.*, vol. 66, no. 1, pp. 763–776, Jan. 2016.

[39] J. Zhang, W. Xiao, Y. Li, S. Zhang, and Z. Zhang, "Multilayer probability extreme learning machine for device-free localization," *Neurocomputing*, vol. 396, pp. 383–393, Jul. 2020.

[40] J. Zhang, Y. Li, W. Xiao, and Z. Zhang, "Non-iterative and fast deep learning: Multilayer extreme learning machines," *J. Franklin Inst.*, vol. 357, no. 13, pp. 8925–8955, 2020.

Jianqiang Xue is currently pursuing the Ph.D. degree with the School of Automation and Electrical Engineering, University of Science and Technology Beijing, Beijing, China.

His research interests include wireless sensor networks and device-free localization.

Jie Zhang (Member, IEEE) received the Ph.D. degree from the University of Science and Technology Beijing, Beijing, China, in 2019.

He was an Associate Professor with the University of Science and Technology Beijing in 2022. From 2019 to 2021, he was a Postdoctoral Research Fellow with Peking University, Beijing. He was a Visiting Research Fellow with the University of Leeds, Leeds, U.K., in 2018, where he is currently a Marie Sklodowska Curie Research Fellow with the School of Electronic and Electrical Engineering. His current research interests include pervasive computing, body sensor networks, wireless sensor networks, and machine learning.

Dr. Zhang was a recipient of the Marie Sklodowska-Curie Actions Individual Fellowships (MSCA-IF), European Commission.

Zhenyue Gao received the M.S. degree from the University of Science and Technology Beijing, Beijing, China, in 2020, where he is currently pursuing the Ph.D. degree in instrument science and technology.

His research interests include machine learning, deep learning, and intelligent sensing.

Wendong Xiao (Senior Member, IEEE) received the Ph.D. degree from Northeastern University, Shenyang, China, in 1995.

He is currently a Professor with the School of Automation and Electrical Engineering, University of Science and Technology Beijing, Beijing, China. Previously, he held various academic and research positions with Northeastern University, POSCO Technical Research Laboratories, Pohang, South Korea; Nanyang Technological University, Singapore; and the Institute for Infocomm Research, A*STAR, Singapore. His current research interests include wearable computing, wireless intelligent sensing, energy-harvesting-based network resource management, and intelligent big data processing.